JOURNAL OF MATERIALS SCIENCE 33 (1998) 5499–5508

Transverse tensile behaviour of fibre reinforced titanium metal matrix composites

M. P. THOMAS, M. R. WINSTONE
Structural Materials Centre, Defence Evaluation and Research Agency, Farnborough, Hampshire, GU14 OLX, UK

Four Ti MMCs have been tested in transverse tension, at ambient temperature and 600 °C. Generally, mechanical properties are reduced compared to monolithic Ti alloys. Transverse Young's modulus is, however, higher than in monolithic alloys, as a result of constraint of the matrix by the fibres.

MMC proportional limits are associated with the onset of interfacial failure. Fibre coating cracking and longitudinal fibre splitting may also contribute to MMC yield and the associated acoustic emission peak. The fibre/matrix interface in IMI 834/SM1140+ appears to be weaker than in the other MMCs, resulting in a lower proportional limit and less acoustic emission. Final failure of the MMCs is generally via ductile shearing of matrix ligaments. The exception to this is IMI 834/SM1140+ in which the matrix fails in a brittle manner. This causes poor transverse tensile strength and failure strain in this MMC.

A model to predict the MMC proportional limit, previously proposed by Jansson *et al.*, has been modified to take account of the tensile strength of the fibre/matrix interface. The model previously used by Jansson *et al.* to predict the transverse tensile strength is acceptably accurate provided that the area fraction of matrix appearing on fracture surfaces is accurately determined.

1. Introduction

Fibre reinforced titanium metal matrix composites (Ti MMCs) are being developed for use in aeronautical gas-turbine engines because of their improved longitudinal specific strength and stiffness and elevated temperature performance compared to monolithic Ti alloys. One of the aero-engine components which would benefit from the incorporation of Ti MMCs is the compressor disc, where reinforcement is obtained via unidirectional, hoop wound SiC fibres. Significant radial and axial stresses can be generated in these discs and it is important, therefore, to characterize the behaviour of unidirectional MMCs subjected to loading at a range of angles to the fibre axis. Presented here are the results of research to characterize the tensile behaviour of four Ti MMCs when subjected to stress perpendicular to the fibre axis, and within the plane of matrix foils and fibre mats (i.e. the transverse orientation).

2. Materials

The MMCs consist of Ti-6Al-4V or IMI 834 (Ti-5.8Al-4.0Sn-3.5Zr-0.7Nb-0.5Mo-0.35Si-0.06C) reinforced with either SM1140+ carbon coated SiC fibre or SM1240 C/TiB_x coated SiC fibre. Panels were produced by the fibre-foil route [1] and were six or eight ply thick. Fibre volume fractions were nominally 0.33. The MMC microstructures have been investigated in detail elsewhere [2]. Rectangular specimens with fibres in the transverse orientation, and dimensions of 10 mm × 150 mm, were electro-discharge machined from the panels, and their edges ground to minimise the effect of machining damage. Protective glass fibre reinforced plastic tabs were bonded to specimen ends.

3. Experimental procedure

Tests were conducted in air, at ambient temperature and 600 °C, at a strain rate of 5.5×10^{-5} s^{-1}, under extension control. Young's modulus was taken as the gradient of the linear, elastic region of stress-strain curves at ambient temperature. At 600 °C, MMC yielding at low strains necessitated the use of the secant moduli method to calculate Young's modulus between 10 MPa and 100 MPa. Acoustic emission from the specimens was detected using a grip-mounted sensor and a 300 kHz to 1 Mhz filter. Specimens of the corresponding monolithic, foil-bonded alloys have previously been tested under identical conditions to act as a comparison [3]. Scanning electron microscopy and energy dispersive X-ray spectroscopy (EDX) have been used to investigate the MMC fracture surfaces.

4. Results and discussion

Table I shows the tensile mechanical properties of the MMCs. The values shown are the mean of four tests and the scatter bands are one standard deviation (σ_n). Data for the monolithic, foil-bonded alloys from [3] are

TABLE I Tensile data obtained from the materials

Material	Test temperature (°C)	Proportional limit (MPa)	Tensile strength (MPa)	Total failure strain (%)	Young's modulus (GPa)
Ti-6Al-4V/	22	275 ± 8	515 ± 2	1.36 ± 0.07	119 ± 5
SM1140+ MMC	600	—	161 ± 10	>5.00	94 ± 5
Ti-6Al-4V/	22	254 ± 11	499 ± 9	0.95 ± 0.06	142 ± 5
SM1240 MMC	600	—	167 ± 6	>5.00	105 ± 5
IMI 834/	22	212 ± 11	265 ± 9	0.24 ± 0.01	119 ± 5
SM1140 + MMC	600	—	165 ± 26	0.43 ± 0.1	98 ± 4
IMI 834/	22	259 ± 9	440 ± 17	0.52 ± 0.07	140 ± 6
SM1240 MMC	600	—	244 ± 4	1.09 ± 0.21	101 ± 6
Foil-bonded	22	862 ± 19	955 ± 7	>5.00	106 ± 1
Ti-6Al-4V*	600	—	285 ± 6	>5.00	49 ± 4
Foil-bonded	22	927 ± 4	994 ± 26	>5.00	109 ± 1
IMI 834*	600	—	472 ± 4	>5.00	56 ± 1

*From reference [3].

also shown. Generally, the mechanical properties of the transverse MMCs are lower than for both the longitudinal orientation [3, 4], and the corresponding monolithic, foil-bonded alloy. This is a result of the minimal influence of the strong, stiff fibres in this orientation, and failure at the weak fibre/matrix interface. Young's moduli of the MMCs are, however, significantly better than in the foil-bonded alloy, as observed in other Ti MMC systems [5]. This is a result of constraint of the matrix between fibres.

At ambient temperature, all MMCs exhibit initial linear, elastic, regions on their stress-strain curves (Fig. 1). It has been suggested that small amounts of local matrix plastic deformation may occur at this stage, but not enough to cause non-linearity [6, 7]. Young's moduli are higher at both temperatures when SM1240 fibre is used. This may be an effect of the different fibre coating materials and thicknesses. Micromechanical modelling has shown that a lower stiffness coating leads to a lower transverse Young's modulus [8]. Also, increasing the thickness of a low stiffness coating decreases this modulus. The SM1140+ fibre has a 5 μm thick carbon coating, whose modulus is likely to be between 20 GPa and 170 GPa, depending on the SiC content [8–11]. The SM1240 fibre has a thinner carbon coating of 1.5 μm and an outer coating of TiB_x, which will have a modulus in the region of 400–500 GPa [11, 12]. Thus, from the work of [8], it is expected that a Ti alloy reinforced with SM1240 fibres will have a higher transverse modulus than the same alloy reinforced with a similar volume fraction of SM1140+ fibres.

As the applied stress approaches 275 MPa, plastic deformation occurs, which is usually attributed to failure of the interface between fibre and matrix [6, 7, 13, 14]. In the current MMCs, with the exception of IMI 834/SM1140+, other mechanisms may also contribute to the proportional limit and the associated acoustic emission peak. In these MMCs a number of sub-fracture surface fibres exhibited longitudinal splitting (Fig. 2). Also, the carbon coating in the Ti-6Al-4V/SM1140+ occasionally exhibited cracking perpendicular to the tensile axis (Fig. 3). These observations suggest that the interface between fibre and matrix has sufficient integrity to transfer enough load to fibres and

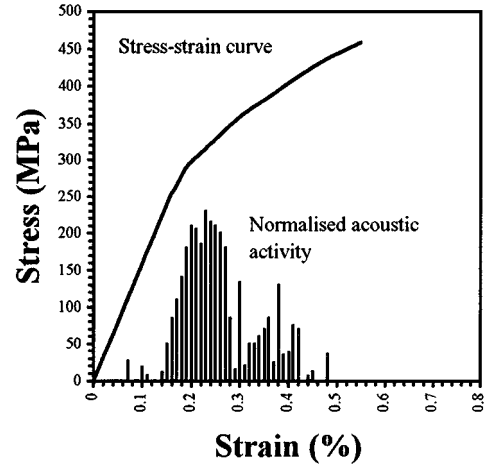

(a)

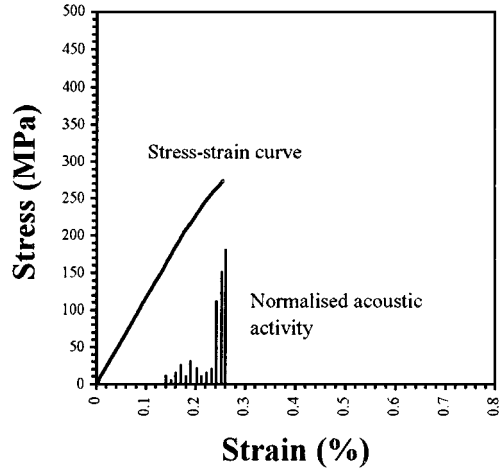

(b)

Figure 1 Representative stress-strain curves for the MMCs at ambient temperature a: IMI 834/SM1240 (Ti-6A1-4V MMCs similar) b: IMI 834/SM1140+.

fibre coatings to cause them to occasionally fail, prior to interfacial failure.

These three MMCs exhibit similar ambient temperature proportional limits. The slight variation between them can be accounted for by differences in the compressive matrix residual stress [3] and interfacial bond strength [15–20] which will affect the applied stress

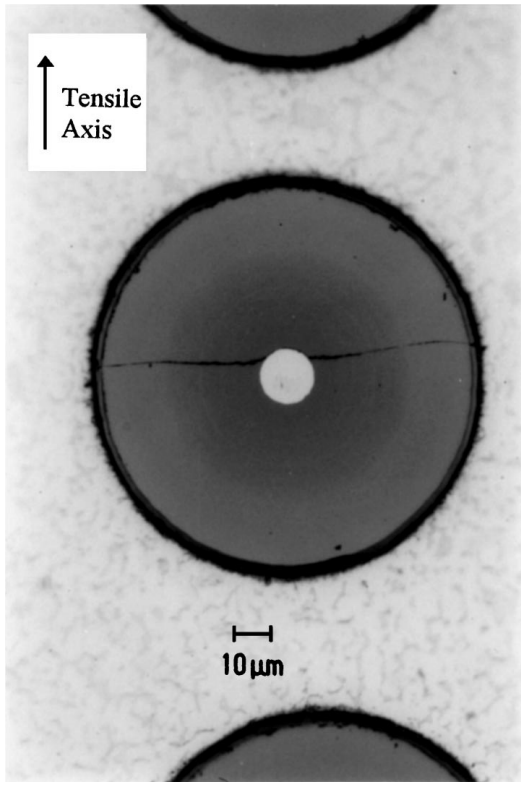

Figure 2 Longitudinal splitting of SiC fibres (Ti-61A1-4V/SM1240 shown).

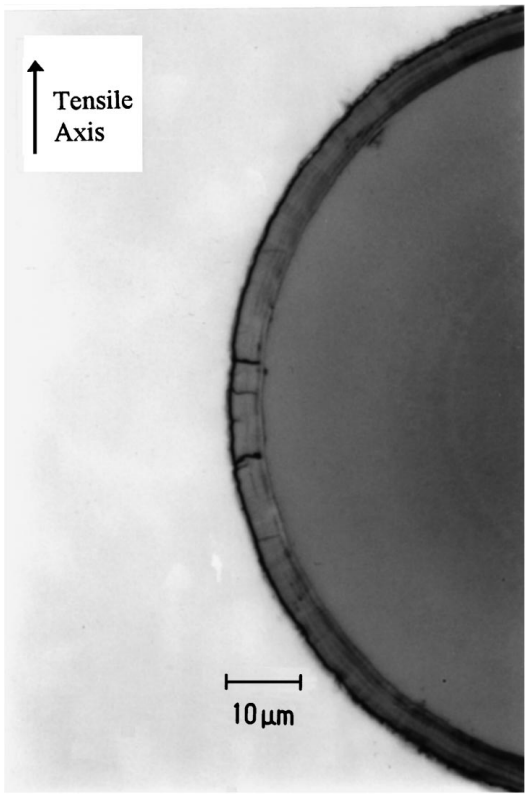

Figure 3 Cracking of carbon coating in Ti-6A1-4V/SM1140+.

required to cause interfacial failure. These MMCs have a proportional limit significantly higher than that measured for an SM1240 fibre reinforced Ti-6242 MMC, tested using similar geometry specimens [21].

Since IMI 834/SM1140+ does not exhibit split fibres nor carbon coating cracking, this MMC may have a low interfacial bond strength. This is further suggested by the fact that the initial yielding is not accompanied by an acoustic emission peak. The proportional limit in IMI 834/SM1140+ is significantly lower than in the other three MMCs. This is surprising since IMI 834/SM1140+ is expected to have the highest compressive matrix residual stress [4] which would result in a high proportional limit. A low interfacial strength or premature failure of the matrix are the most logical explanations of the poor proportional limit.

In Ti-6Al-4V/SM1240, interfacial failure occurs either through the carbon coating, often between the two distinct carbon layers (Fig. 4) or the TiB/TiB_2 reaction layer. This interfacial failure position has been noted previously [22]. Interfacial failure in IMI 834/SM1240 is slightly different, rarely occurring within the carbon layer. The favoured failure positions for this MMC are the interface between the carbon coating and the TiB/TiB_2 reaction layer, or within the TiB/TiB_2 reaction layer itself.

Interfacial failure in Ti-6Al-4V/SM1140+ occurs either at the carbon/TiC reaction layer interface, or between the layers of the carbon coating (Fig. 5). Interfacial failure in IMI 834/SM1140+ occurs exclusively between the fibre carbon coating and the TiC reaction layer (arrow “a” on Fig. 6) producing the fracture surface as seen in Fig. 7. The position of interfacial failure in IMI 834/SM1140+ indicates that this interface is weaker than in Ti-6Al-4V/SM1140+. A similar interfacial failure location has been observed in a variety of Ti matrices reinforced with the SCS-6 fibre [23–25].

In IMI 834/SM1140+ (Fig. 1b), at strains slightly beyond the proportional limit, acoustic emission suddenly increases followed almost immediately by specimen failure. These acoustic events appear to be associated with cleavage cracking of the matrix which initiates at or near the TiC reaction layer (arrow “b” on Fig. 6). The premature failure of IMI 834/SM1140+, which results in a poor tensile strength and failure strain, is caused by rapid joining of these cleavage cracks. Fracture surfaces clearly show large areas of matrix cleavage failure (Fig. 7). Such cleavage has been observed during longitudinal tensile testing of this MMC [3], and is possibly due to a high matrix carbon content caused by carbon diffusion during MMC consolidation [2]. It is suggested that this could lead to an increase in hardness and a decrease in ductility of the matrix, ideal conditions for the inducement of cleavage failure. The predicted high matrix residual stress in IMI 834/SM1140+ may also contribute to the cleavage failure.

In the other three MMCs, the acoustic emission drops as interfacial failure becomes exhausted. Here, plastic deformation towards the end of the stress-strain curve is caused by elongation of matrix ligaments between fibres [6, 7, 13, 14], which fail by ductile void coalescence. The tensile strengths of the two Ti-6Al-4V MMCs are similar and are significantly better than that previously measured for Ti-6Al-4V/SM1140+ [14]. IMI 834/SM1240 has an ambient temperature strength lower than the Ti-6Al-4V matrix MMCs. This can be

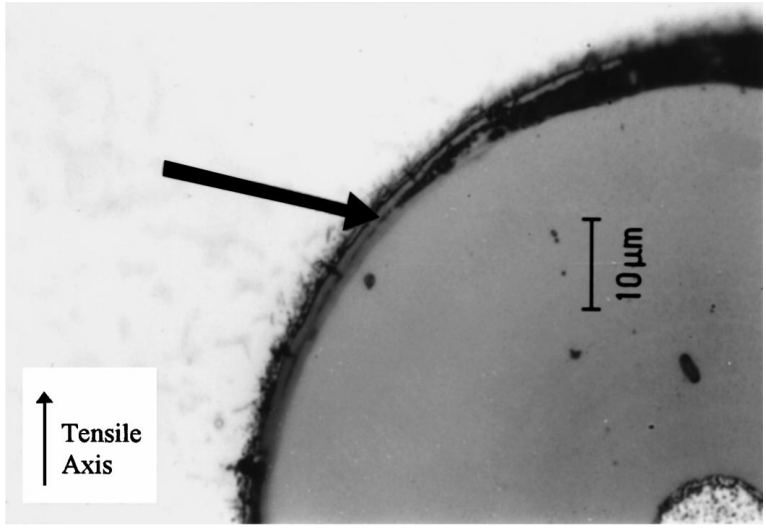

Figure 4 Interfacial failure between carbon layers (arrowed) in Ti-6Al-4V/SM1240.

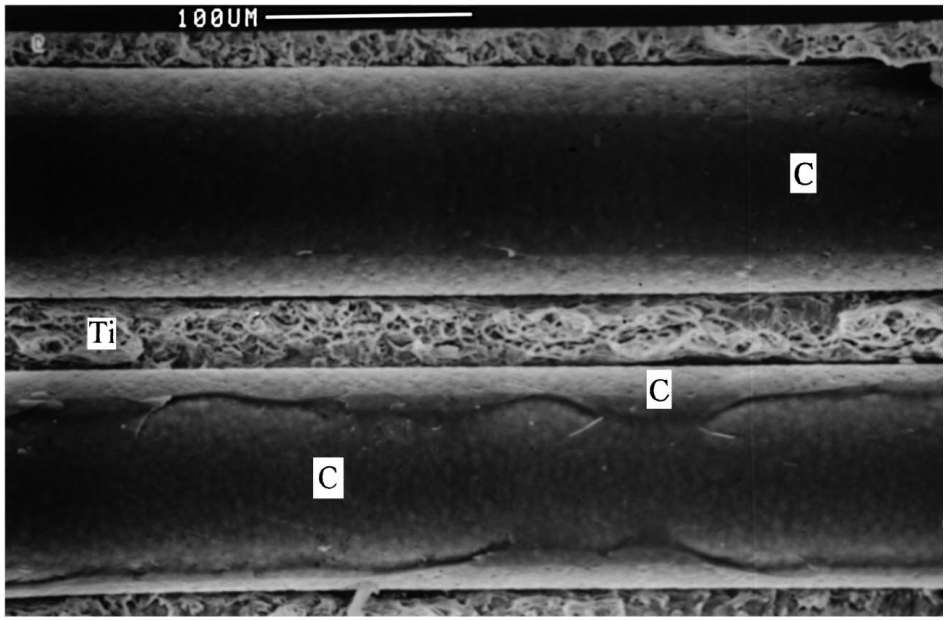

Figure 5 Fractograph of Ti-6A1-4V showing interfacial failure (species identified by EDX).

accounted for by differences in the fibre packing and panel geometry, as will be shown in section 5.2

Although better than IMI 834/SM1140+, the failure strains of these three MMCs are significantly lower than those of the monolithic, foil-bonded alloys because of matrix constraint and matrix tensile residual stress between fibres in the loading direction. The Ti-6Al-4V MMCs have failure strains significantly higher than both IMI 834 MMCs at both testing temperatures, because of their lower tensile matrix residual stress. In addition, the IMI 834 matrix contains large numbers of silicide particles [2] which are known to reduce the ductility of this alloy [26].

At 600 °C, the MMCs do not show a linear, elastic region on stress-strain curves, but display a small amount of yielding from load-up (Fig. 8). Proportional limits could not be calculated, therefore, at this temperature. This non-linearity has previously been attributed to interfacial failure, as a result of relaxation of matrix residual stress [27]. It is likely, however, that this initial MMC yielding is predominantly due to yielding of the matrix alloy, which occurs at very low stress at this high temperature [3]. This is suggested because interfaces do, in fact, have an inherent tensile strength and are not simply held together by residual stress [28, 29]. Even though the initial portion of stress-strain curves is non-linear, a definite change in gradient is observed at approximately 80 MPa which, in the Ti-6Al-4V MMCs and the IMI 834/SM1240, is accompanied by the onset of acoustic emission (Fig. 8a). These observations suggest that it is at this stress that interfacial failure initiates, not immediately on load up as suggested in [27]. The mechanisms of plastic deformation and final failure are the same in these MMCs at this temperature as they are at ambient temperature, but IMI 834 / SM1240 has superior tensile strength to the Ti-6Al-4V MMCs, due to the inherently better elevated temperature properties of the IMI 834 matrix alloy.

In IMI 834/SM1140+, similar observations are made at 600 °C as were made at ambient temperature.

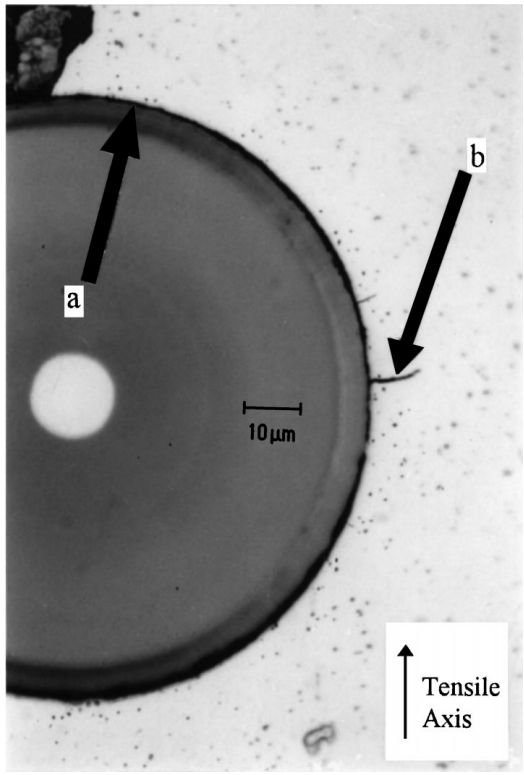

Figure 6 Interfacial separation (arrow "a") and matrix cracking (arrow "b") in IMI 834/SM1140+.

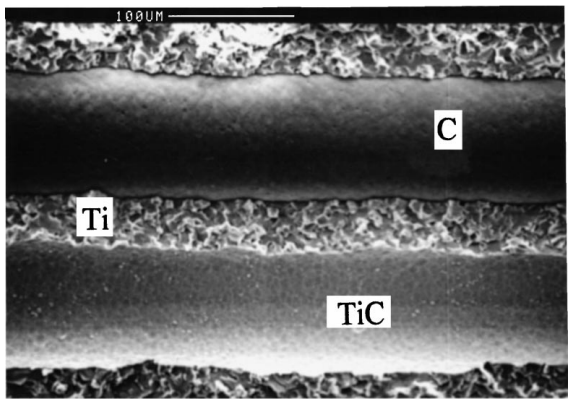

Figure 7 Fracture surface of IMI 834/SM1140+ failure (species identified by EDX).

Yielding, attributed to interfacial failure, is not accompanied by acoustic emission (Fig. 8b), and specimen failure again appears to be due to matrix cleavage cracking. At 600 °C, specimen failure is also influenced by intergranular matrix failure, which occurs near the specimen surface (Fig. 9). Intergranular damage has been observed in this MMC after longitudinal tensile and creep testing at 600 °C and is attributed to oxidation [3, 30]. Such damage is absent in the SM1240 fibre reinforced MMCs, but is present to a small extent in Ti-6Al-4V/SM1140+. This suggests that it may be an effect of oxidation interacting with carbon present in the matrix. At this temperature the tensile strength of IMI 834/SM1140+ is similar to the Ti-6Al-4V MMCs, because the matrix embrittlement and superior elevated temperature properties of the IMI 834 matrix effectively cancel each other out.

At 600 °C, MMC failure strains are improved over their ambient temperature values because of relaxation

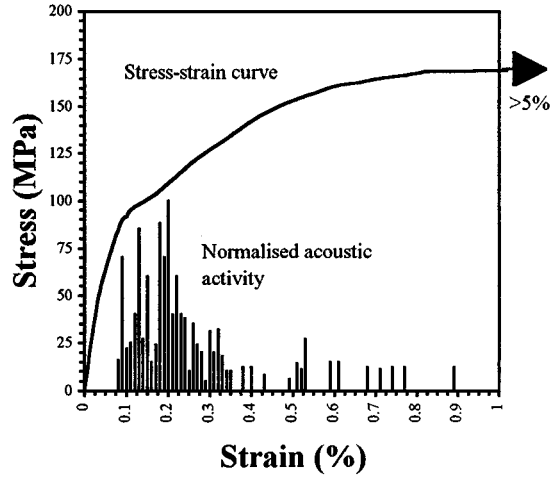

(a)

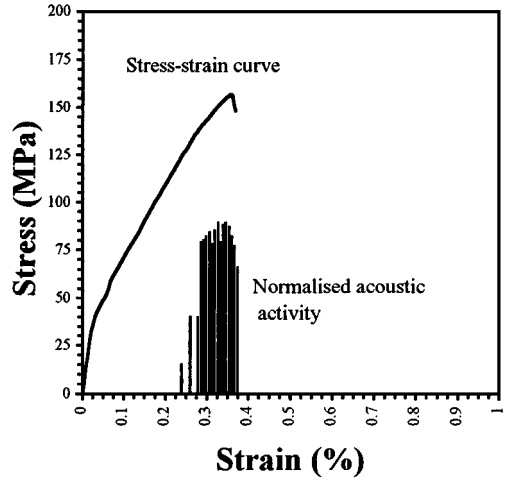

(b)

Figure 8 Representative stress-strain curves of the MMCs at 600 °C a: Ti-6A1-4V/SM1140+ (SM1240 reinforced MMCs similar) b: IMI 834/SM1140+.

of matrix residual stress (partial relaxation in the case of the IMI 834 matrix). At this temperature the failure strains of the Ti-6Al-4V MMCs exceeded the limit of the extensometer (5%) due to the onset of creep. For these specimens the failure strains are unknown.

In all the MMCs, tested at 600 °C, oxidation has penetrated approximately 500 μm along the interfaces of surface exposed fibres, causing damage to the fibre coating (Fig. 10). Such damage is known to embrittle the interfacial region and lead to a reduction in mechanical properties [31–33]. This effect was observed to an equal extent in all the MMCs, however, and so cannot account for differences in their mechanical performance.

5. Modelling of mechanical properties

5.1. Proportional limit

Jansson et al. proposed a model whereby the MMC was said to yield as soon as the matrix residual stresses, which clamp the fibre/matrix interface shut, were overcome by the applied stress [13]. This model assumes, therefore, that interfaces have zero tensile strength. From the equations of Jansson et al., this model can be written as:

$$\sigma_{pl} = \sigma_r \Bigg/ \left[\frac{11 - 17\nu_m + 6\nu_f^2 + \frac{G_m}{G_f}(9 - 14\nu_f - 9\nu_m + 14\nu_m\nu_f)}{5 - 6\nu_m + \frac{G_m}{G_f}(8 - 12\nu_f - 6\nu_m + 12\nu_m\nu_f) + \left(\frac{G_m}{G_f}\right)^2 (3 - 8\nu_f + 4\nu_f^2)} \right] \quad (1)$$

where:

σ_{pl} = MMC proportional limit
σ_{r} = Matrix radial thermal residual stress
ν_{m} = Matrix alloy Poissons ratio
ν_{f} = Fibre Poissons ratio
G_{m} = Matrix alloy shear modulus
G_{f} = Fibre shear modulus

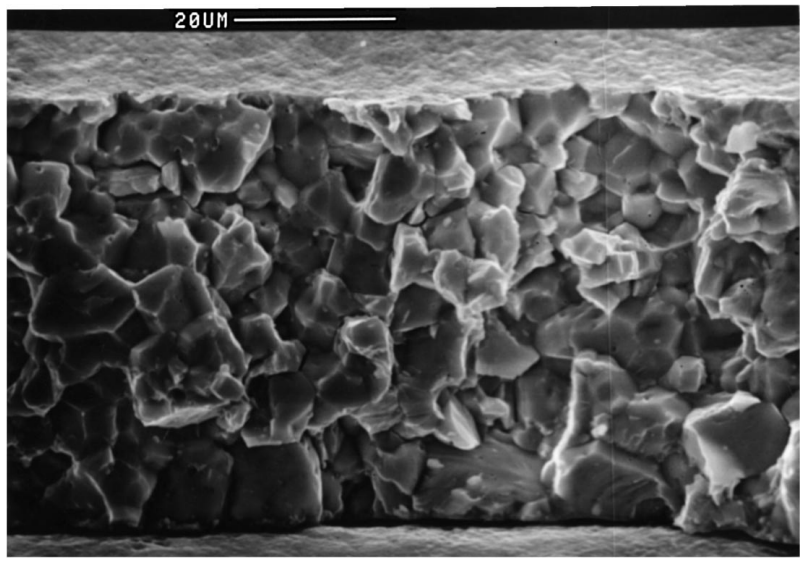

Figure 9 Intergranular matrix failure in IMI 834/SM1140+ tested at 600 °C.

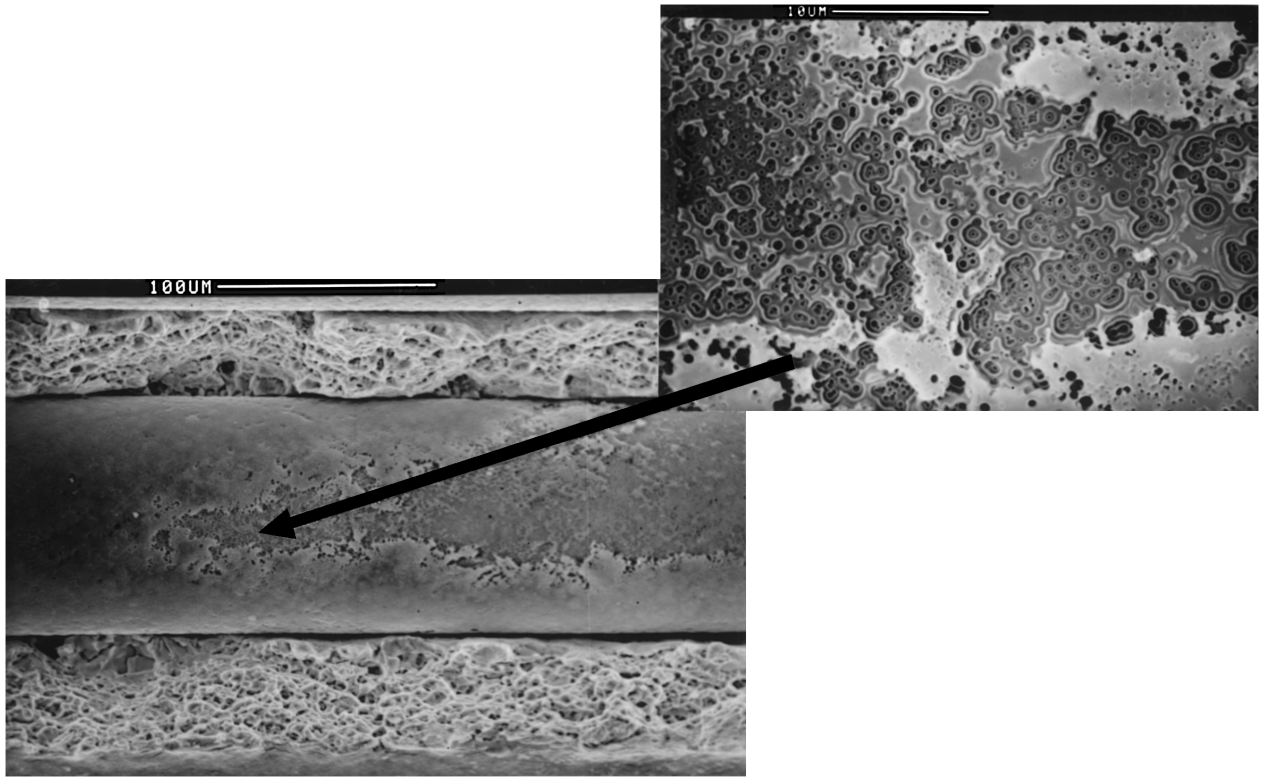

Figure 10 Near-surface oxidation of fibre coating (IMI 834/SM1140+ shown, but all MMCs similar).

Input values were taken as: $\nu_m = 0.33$ [13], $\nu_f = 0.17$ [13], $G_m = 45$ GPa [34, 35], $G_f = 202$ GPa [35]. This reduces equation (1) to:

$$\sigma_{pl} = \frac{\sigma_r}{1.58} \tag{2}$$

This equation has previously been found to accurately predict the proportional limit of an SCS-6 fibre reinforced Ti-15-3 MMC [13]. Miracle et al. have used a similar equation to model a Ti-6242/SM1240 MMC [21] with some success. It is noted, however, that the values of matrix residual stress used in these papers (−300 MPa for the Ti-15-3 matrix [13] and −420 MPa for the Ti-6242 matrix [36]) are rather high. If more realistic values of matrix residual stress for these two systems [14, 37–41] are used in Equation 2, the proportional limit is severely underestimated.

A mean literature value of matrix radial residual stress in a Ti-6Al-4V alloy reinforced with carbon coated fibres is −237 MPa [42–45]. If this value is used for the current Ti-6Al-4V/SM1140+ MMC then, once again, the proportional limit is underestimated by Equation 2.

It is suggested that the failure of Equation 2 to predict the proportional limit of MMCs, when a realistic value of radial matrix residual stress is used, is due to the assumption that the interface has no inherent tensile strength. Measurements of interfacial shear strength [15–20] would suggest that this is not so and, indeed, preliminary work shows that the interfacial tensile strength in SCS-6 reinforced Ti-6Al-4V is of the order of 145 MPa [28, 29]. Thus, the interfacial tensile strength has to be overcome as well as the matrix residual stress, before interfacial failure occurs. Equation 2 must be modified to:

$$\sigma_{pl} = \frac{\sigma_r + \sigma_i}{1.58} \tag{3}$$

where: σ_i = Interfacial tensile strength.

If Equation 3 is used for the current Ti-6Al-4V/SM1140+, with the value of interfacial tensile strength found in [28, 29], it predicts a proportional limit of 242 MPa which is close to the experimental value of 275 MPa. This seems to vindicate the assumption that the interface has a tensile strength which affects the MMC proportional limit.

Equation 3 cannot currently be used to calculate the proportional limit of the other MMCs since the radial matrix residual stress in these MMCs has not been calculated, and the tensile interfacial strength has not been estimated for the SM1240 fibre. The interfacial shear strength for Ti-6Al-4V reinforced with SM1240 fibres has been calculated, however, as 103 MPa [46].

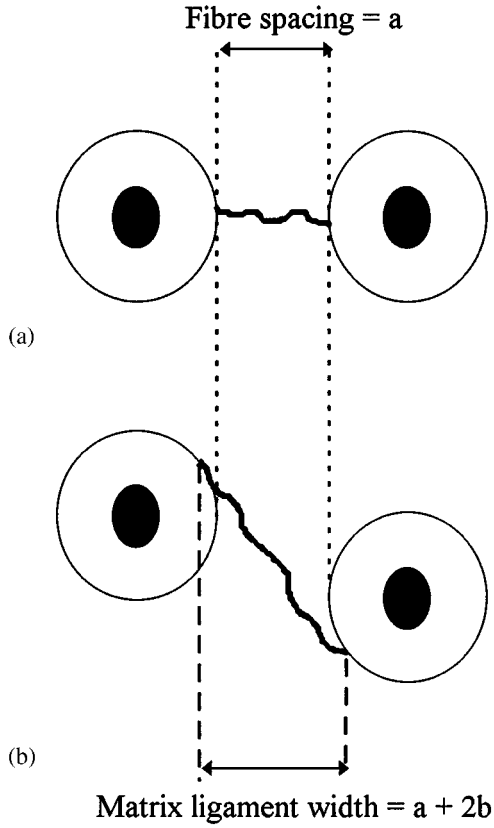

Figure 11 Schematic of matrix fracture path and ligament dimensions for use in equations (6) and (7) a. IMI 834/SM1140+ b. All other MMCs, in which matrix failure is via shearing.

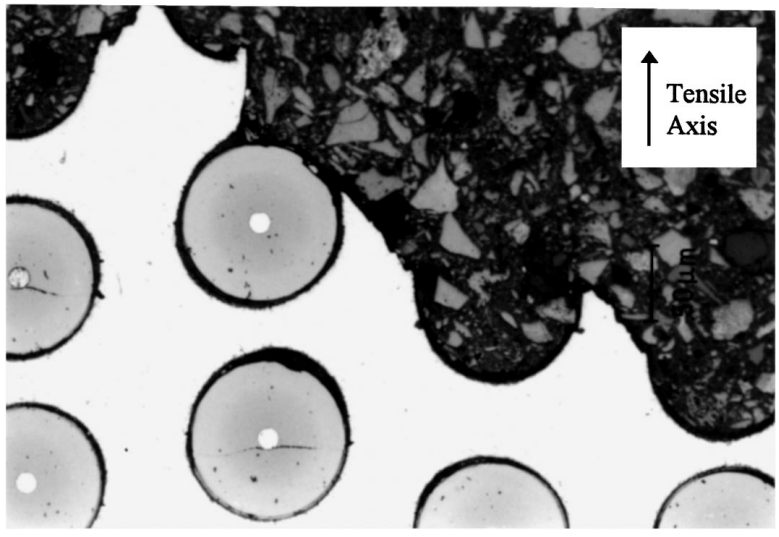

Figure 12 Shear failure of matrix ligaments as seen in all MMCs, except IMI 834/SM1140+.

This can be used to estimate the interfacial tensile strength as [47]:

$$\sigma_i = 1.7 * \tau_i \tag{4}$$

where: τ_i = Interfacial shear strength.

Knowing the value of interfacial tensile strength from Equation 4, Equation 3 can be used "in reverse" to estimate the radial matrix thermal stress in the Ti-6Al-4V/SM1240 MMC:

$$254 = \frac{\sigma_r + (1.7 * 103)}{1.58} \qquad \text{Thus, } \sigma_r = -226\,\text{MPa}$$

The interfacial fracture behaviour of the IMI 834/SM1240 is similar to that of the Ti-6-4/SM1240 so it may be assumed that the interfacial strength is similar. Equations 3 and 4 then predict that the matrix radial residual stress in the IMI 834/SM1240 is −244 MPa. The interfacial failure behaviour of the IMI 834/SM1140+ suggests that the interface has minimal strength. If the interfacial tensile strength is set to zero then the matrix radial residual stress is calculated from Equations 3 and 4 as −335 MPa.

Equation 3 predicts that the IMI 834 MMCs have radial matrix residual stresses higher than the Ti-6Al-4V MMCs, and that MMCs reinforced with SM1240 fibre will have lower residual stress than those reinforced with SM1140+ fibre. These trends are to be expected if the relative properties of the two matrix alloys and the two fibre coatings are considered [4].

5.2. Tensile strength

Since transverse failure of MMCs is caused by failure of matrix ligaments, Jansson *et al*. proposed a model based on a function of the matrix strength and the area fraction of matrix present on fracture surfaces [13, 48]:

$$\sigma_{\text{uts}} = A_m \frac{2}{\sqrt{3}} \sigma_{m,uts} \tag{5}$$

where:

σ_{uts} = MMC ultimate tensile strength
A_m = Area fraction of matrix on fracture surfaces
$\sigma_{m,uts}$ = Ultimate tensile strength of matrix alloy

The main difficulty with this equation is assigning an accurate value for the area fraction of matrix on fracture surfaces. Since the matrix will fail at the minimum width of the ligaments between fibres, it might be expected that the fracture would follow the path in Fig. 11a for a square packed fibre array. This is true of the IMI 834/SM1140+ MMC, in which significant amounts of the matrix fail by cleavage, and shear is minimal. In this case, the area fraction of matrix on the fracture surface can be calculated from:

$$A_m = \frac{T - (P_f * D_f)}{T} \tag{6}$$

where

T = Specimen thickness
P_f = Number of fibre plies in the MMC panel
D_f = fibre diameter

For the other three MMCs, however, significant shearing of the matrix occurs during ligament failure. Also the fibre packing is often hexagonal rather than square [2]. This results in the fracture surface morphology shown in Fig. 12. This is drawn schematically in Fig. 11b. The shearing and fibre placement result in the matrix ligaments being wider than in the IMI 834/SM1140+. Thus, the area fraction of matrix on the fracture surface of these MMCs is given by:

$$A_m = \frac{T - [P_f * (D_f - 2b)]}{T} \tag{7}$$

Extensive measurement of sections taken through fracture surfaces indicates that, in the MMCs which exhibit significant shearing of the matrix, b ≈ 8 μm.

Equations 6 and 7 have been used to calculate the area fractions of matrix predicted to appear on the fracture surface of each MMC. The values obtained, together with the resulting prediction of MMC transverse strength from Equation 5, are shown in Table II. Equations 5 to 7 provide a good estimate for the tensile strength of the MMCs at both temperatures, with the exception of the IMI 834/SM1140+, at ambient temperature. Although equation (5) predicts, correctly, that the IMI 834/SM1140+ will have the lowest tensile strength it overestimates the value, because it does not take account of the matrix embrittlement

TABLE II Comparison of predicted and experimental transverse tensile strength

Material	Area fraction of matrix on fracture surface (A_m)$^+$	Temperature (°C)	Matrix Tensile Strength (MPa)*	MMC Tensile Strength from Equation 4 (MPa)	MMC Experimental Tensile Strength (MPa)
Ti-6-4/	0.45	22	955	497	501
SM1240		600	285	148	167
Ti-6-4/	0.46	22	955	510	515
SM1140+		600	285	152	161
IMI 834/	0.42	22	994	482	444
SM1240		600	472	229	244
IMI 834/	0.33	22	994	375	265
SM1140+		600	472	178	165

$^+$Obtained from Equations 6 and 7.
*Taken from reference [3].

present in this MMC. In this case a modified value of the matrix tensile strength should be used in Equation 5.

6. Conclusions

1. Transverse Young's modulus of the MMCs is superior to that of the corresponding monolithic, foil-bonded alloy at both testing temperatures, because of constraint of the matrix between fibres. All other properties are, however, significantly worse than foil-bonded alloys.

2. Young's modulus of the MMCs reinforced with SM1240 fibres is higher than that of the MMCs reinforced with SM1140+ fibres. This is attributed to differences in the stiffness and thickness of the fibre coatings.

3. The proportional limit in these MMCs is caused by the onset of fibre/matrix interfacial failure. Fibre splitting and fibre coating cracking may also contribute.

4. The fibre/matrix interface in the IMI 834/SM1140+ appears to be significantly weaker than that in the other MMCs.

5. Final failure of the MMCs is usually by ductile shearing of matrix ligaments between fibres. The one exception to this is the IMI 834/SM1140+ in which the matrix fails in a brittle manner, causing a low tensile strength and poor failure strain.

6. Models to predict the proportional limit in transverse MMCs need to be modified to take account of the intrinsic tensile strength of the interface.

7. The transverse tensile strength of the MMCs is adequately predicted using the model previously used by Jansson et al, provided that the area fraction of matrix on fracture surfaces is accurately calculated.

Acknowledgements

British Crown Copyright 1998/DERA. Published with the permission of the controller of Her Britannic Majesty's Stationary Office.

The authors gratefully acknowledge support from the MOD Applied Research Programme, and from the DTI CARAD programme.

References

1. J. G. ROBERTSON in "Characterisation of Fibre Reinforced Titanium Matrix Composites" – AGARD Report No. 796 (NATO Advisory Group for Aerospace Research and Development, Neuilly-sur-Seine, France, 1994) pp. 7.1–7.8.
2. M. P. THOMAS, J. G. ROBERTSON and M. R. WINSTONE, *J. Mat. Sci*. Vol. 33 (1998) pp. 3607–3614.
3. M. P. THOMAS and M. R. WINSTONE, *Scripta Materialia* Vol. 37 (1997) pp. 1855–1862.
4. M. P. THOMAS and M. R. WINSTONE, "Longitudinal Yielding Behaviour of SiC Fibre Reinforced Titanium Matrix Composites," To be published in *Composites Science & Technology*, 1998.
5. W. S. JOHNSON, S. J. LUBOWINSKI and A. L. HIGHSMITH, in "Thermal and Mechanical Behaviour of Metal Matrix and Ceramic Matrix Composites," ASTM STP-1080. Edited by: J. M. Kennedy, H. H. Moeller and W. S. Johnson (American Society for Testing and Materials, Philadelphia, 1990) pp. 193–218.
6. B. S. MAJUMDAR and G. M. NEWAZ, *Phil. Mag*. Vol. 66 (1992) pp. 187–212.
7. J. G. BAKUCKAS, W. H. PROSSER and W. S. JOHNSON, *J. Comp. Mat*. Vol. 28 (1994) pp. 305–328.
8. D. S. LI and M. R. WISNOM, *J.Comp.Mat*. Vol. 30 (1996) pp. 561–588.
9. R. A. SHATWELL, *Mat. Sci. Tech*. Vol. 10 (1994) pp. 552–557.
10. C. L. MANTELL, in "Carbon and Graphite Handbook" (Interscience Publishers, London, 1968) pp. 22–27.
11. J. E. HOVE and W. C. RILEY, in "Ceramics for Advanced Technologies" (John Wiley & Son, London, 1965) pp. 17, 23, 61, 158.
12. K. L. CHOY, J. F. DURODOLA, B. DERBY and C. RUIZ, *Composites* Vol. 26 (1995) pp. 531–539.
13. S. JANSSON, H. E. DÈVE and A. G. EVANS, *Met. Trans*. Vol. 22A (1991) pp. 2975–2984.
14. P. J. COTTERILL and P. BOWEN, *J. Mat. Sci*. Vol. 31 (1996) pp. 5897–5905.
15. J. M. YANG, S. M. JENG and C. J. YANG, *Mat. Sci. Eng*. Vol. A138 (1991) pp. 155–167.
16. L. MOLLIEX, J. P. FAVRE, A. VASSEL and M. RABINOVITCH, *J. Mat. Sci*. Vol. 29 (1994) pp. 6033.
17. Y. LEPETITCORPS, R. PAILLER and R. NASLAIN, *Comp. Sci. Tech*. Vol. 35 (1989) pp. 207–214.
18. M. C. WATSON and T. W. CLYNE, in "Titanium '92: Science and Technology." Edited by: F. H. Froes and I. Caplan (The Minerals, Metals and Materials Society, Pennsylvania, 1993) pp. 2569–2576.
19. Z. X. GUO and B. DERBY in "Titanium '92: Science and Technology." Edited by: F. H. Froes and I. Caplan (The Minerals, Metals and Materials Society, Pennsylvania, 1993) pp. 2633–2640.
20. M. C. WATSON and T. W. CLYNE, *Acta Met.& Mat*. Vol. 40 (1992) pp. 141–148.
21. D. B. MIRACLE, A. F. KALTON and T. W. CLYNE, in "Proceedings of ICCM-11: The Eleventh International Conference on Composite Materials." Vol. III Edited by: M. L. Scott (Australian Composite Structures Society, Melbourne, 1997) pp. 317–326
22. D. UPADHYAYA, B. BRYDSON, C. M. WARD-CLOSE, P. TSAKIROPOULOS and F. H. FROES, *Mat. Sci. Tech*. Vol.10 (1994) pp. 797–806.
23. T. P.GABB, J. GAYDA and R. A. MACKAY, *J. Comp. Mat*. Vol. 24 (1990) pp. 667–686.
24. D. E. MOREL, in "Titanium '92: Science and Technology." Edited by: F. H. Froes and I. Caplan (The Minerals, Metals and Materials Society, Pennsylvania, 1993) pp. 2553–2560.
25. C. JONES, C. J. KIELY and S. S. WANG, *J. Mat. Res*. Vol. 5 (1990) pp. 1435–1442.
26. A. P. WOODFIELD, M. H. LORETTO and R. E. SMALLMAN, in "Titanium: Science and Technology." Vol. 3. Edited by: G. Lutjering, U. Zwicker and W. Bunk (Deutsche Gesellschaft fur Metallkunde E. V., Oberursel, Germany, 1985) pp. 1527–1534.
27. B. S. MAJUMDAR, G. M. NEWAZ, F. W. BRUST and J. R. ELLIS, in "Titanium '92: Science and Technology." Edited by: F. H. Froes and I. Caplan (The Minerals, Metals and Materials Society, Pennsylvania, 1993) pp. 2609–2616.
28. D. B. GUNDEL, B. S. MAJUMDAR and D. B. MIRACLE, *Scripta Materialia* Vol. 33 (1995) pp. 2057–2065.
29. S. G. WARRIER, B. S. MAJUMDAR, D. B. GUNDEL and D. B. MIRACLE, *Acta Materialia* Vol. 45 (1997) pp. 3469–3480.
30. M. P. THOMAS, J. G. ROBERTSON, B. MORGAN and M. R. WINSTONE, in "Titanium '95." Vol. III. Edited by: P. A. Blenkinsop et al (Institute of Materials, London, 1996) pp. 2811–2818.
31. W. WEI, *J. Mat. Sci*. Vol. 27 (1992) pp. 1801–1810.
32. N. LEGRAND, J. GRISON and L. REMY in "Fatigue '96: Proceedings of the Sixth International Fatigue Congress." Vol. III. Edited by: G. Lutjering and H. Nowack (Pergamon Press, Oxford, 1996) pp. 1451–1456.
33. M. G. EGGLESTON and A. M. RITTER, *Met. & Mat. Trans*. Vol. 26A (1995) pp. 2733–2744.
34. E. W. COLLINGS, in "The Physical Metallurgy of Titanium Alloys." (ASM, Ohio, 1984) pp. 116.
35. K. S. CHAN and D. L. DAVIDSON, *Eng. Fract. Mech*. Vol. 33 (1989) pp. 451–466.

36. W. S. JOHNSON, in "Damage Development in Titanium Metal Matrix Composites Subjected to Cyclic Loading," NASA Technical Memorandum 107597 (NASA Langley, Virginia, 1992).
37. J. GAYDA, T. P. GABB and A. D. FREED, "The Isothermal Fatigue Behaviour of a Unidirectional SiC/Ti Composite and the Ti Alloy Matrix," NASA Technical Memorandum 101984 (NASA Lewis Research Center, Ohio, April 1989).
38. W. S. JOHNSON, R. A. NAIK and W. D. POLLOCK, in "Fatigue '90" (Materials and Component Engineering Publications Ltd., Birmingham, 1991) pp. 841–850.
39. S. MALL and P. G. ERMER, *J. Comp. Mat*. Vol. 25 (1991) pp. 1668–1686.
40. P. RANGASWAMY, M. A. M. BOURKE, P. K. WRIGHT, N. JAYARAMAN, E. KARTZMARK and J. A. ROBERTS, *Mat. Sci. Eng*. Vol. A224 (1997) pp. 200–209.
41. J. JO, S. PARTHASARATHI, V. RAMNARAYAN, R. E. SWANSON and J. PARNELL, in "Residual Stresses in Composites: Measurement, Modelling and Effects on Thermo-Mechanical Behaviour." Edited by: E. V. Barrera and I. Dutta (The Minerals, Metals & Materials Society, Pennsylvania, 1993) pp. 219–226.
42. G. F. HARRISON, B. MORGAN, P. H. TRANTER and M. R. WINSTONE, in "Characterisation of Fibre Reinforced Titanium Matrix Composites," AGARD Report No. 796 (NATO-AGARD, Neuilly-sur-Seine, France, 1994) pp. 14.1–14.15.
43. J. B. BRAYSHAW and M. J. PINDERA, in "Mechanics of Composites at Elevated and Cryogenic Temperatures" (ASME, New York, 1991) pp. 23–37.
44. J. F. DURODOLA and C. RUIZ, in "Advanced Composites '93: International Conference on Advanced Composite Materials." Edited by: T. Chandra and A. K. Dhingra (The Minerals, Metals and Materials Society, Pennsylvania, 1993) pp. 1133–1139.
45. D. UPADHYAYA, D. M. BLACKLETTER and F. H. FROES, in "Titanium '92: Science and Technology," Vol. III. Edited by: F. H. Froes and I. L. Caplan, (The Minerals, Metals and Materials Society, Pennsylvania, 1993) pp. 2537–2543.
46. J. GAYDA and T. P. GABB, *Int. J. Fat*. Vol. 14 (1992) pp. 14–20.
47. G. E. DIETER, in "Mechanical Metallurgy" (McGraw-Hill, London, 1984) pp. 80.
48. S. JANSSON, D. J. DAL BELLO and F. A. LECKIE, *Act Met. & Mat.* Vol. 42 (1994) pp. 4015–4024.

Received 18 June
and accepted 21 July 1998